Vol. 522: 33–48, 2015
doi: 10.3354/meps11118

MARINE ECOLOGY PROGRESS SERIES
Mar Ecol Prog Ser

Published March 2

Coral reef benthic regimes exhibit non-linear threshold responses to natural physical drivers

Jamison M. Gove[1,6,*,], Gareth J. Williams[2,**], Margaret A. McManus[3], Susan J. Clark[1,4], Julia S. Ehses[1,4], Lisa M. Wedding[5]**

[1]Coral Reef Ecosystem Division, NOAA Pacific Islands Fisheries Science Center, Honolulu, Hawai'i 96818, USA
[2]Center for Marine Biodiversity and Conservation, Scripps Institution of Oceanography, La Jolla, California 92083, USA
[3]School of Ocean and Earth Science and Technology, University of Hawai'i at Mānoa, Honolulu, Hawai'i 96822, USA
[4]Joint Institute for Marine and Atmospheric Research, University of Hawai'i at Mānoa, Honolulu, Hawai'i 96822, USA
[5]Center for Ocean Solutions, Stanford University, Monterey, California 93940, USA
[6]*Present address:* Ecosystems and Oceanography Division, NOAA Pacific Islands Fisheries Science Center, Honolulu, Hawai'i 96818, USA

ABSTRACT: We assessed the independent effects of natural physical drivers in structuring coral reef benthic communities at a remote oceanic atoll in the central equatorial Pacific with minimal local human impacts. High-resolution bathymetric data combined with *in situ* oceanographic measurements and a nearshore hydrodynamic model revealed complex intra-atoll gradients in geomorphic complexity, wave forcing, currents, and temperature. For example, maximum wave-driven bed shear stress spatially varied on the forereef (15–20 m depth) by over 2 orders of magnitude, peaking in areas exposed to multiple wave regimes. Benthic community composition, quantified via towed-diver imagery collected in a complete circumnavigation of the atoll (~40 km), also exhibited considerable spatial heterogeneity. Benthic competitors showed distinct, non-linear threshold-type responses to variations in physical drivers. For example, at a wave-driven bed shear stress threshold of 18 N m^{-2}, calcifying crustose coralline algae lost relative dominance and were replaced by non-calcifying fleshy turf algae. Hard coral communities also demonstrated considerable flexibility in response to physical drivers, with distinct shifts in the relative dominance of different growth morphologies along gradients of wave forcing, presumably as a means of local adaptation. Our results highlight (1) the importance of natural gradients in physical drivers in determining dominant benthic regimes on coral reefs (e.g. calcifying vs. fleshy), (2) that non-linear thresholds (or tipping points) exist between key benthic competitors in response to key physical drivers, and (3) that coral assemblages show inherent flexibility and can reorganize in response to physical drivers rather than exhibit wholesale changes in overall cover.

KEY WORDS: Coral morphology · Regime shift · Reef-building organisms · Competition · Habitat complexity · Biophysical coupling · Waves · Bed shear stress · Tipping points

INTRODUCTION

Natural physical drivers structure coral reef benthic communities across a range of spatial scales. The global latitudinal range in temperature restricts the geographic extent of tropical coral reefs at the broadest spatial scale (Kleypas et al. 1999), while at the finest spatial scale (e.g. at the scale of individual reef-building organisms), water motion regulates benthic boundary layer dynamics, mediating mass transfer and nutrient uptake for corals and algae (Atkinson & Bilger 1992, Thomas & Atkinson 1997). Long-term background physical conditions drive clear spatial patterning in benthic communities and dominant

*Corresponding author: jamison.gove@noaa.gov
**These authors contributed equally to this work

morphological traits owing to local community adaptation (Brown 1997, Done 1999, Hughes et al. 2012, Williams et al. in press). Superimposed over these naturally coupled biophysical relationships are episodic disturbance events (e.g. hurricanes) that shift entire communities to earlier successional states (Sousa 1984). The combined effects of mean background conditions and anomalous events are key structuring forces that drive community dynamics, competitive outcomes, and thus the relative dominance of benthic organisms at any one point in time (Littler & Littler 1985, Hughes & Connell 1999).

At the scale of individual islands and coral atolls, gradients in physical drivers are largely determined by interactions of waves and currents with underlying bathymetry. For example, ocean current–bathymetric interactions can lead to vertical transport of oceanic water masses (Hendry & Wunsch 1973, Hamann et al. 2004), delivering sub-thermocline, nutrient-laden waters to shallow-water benthic coral reef communities (Andrews & Gentien 1982). Similarly, tidal currents that hit steep-sided islands and atolls can drive localized, high-frequency variations in water flow, temperature, nutrients, and suspended particles (Wolanski & Delesalle 1995, Leichter et al. 1998) that can influence coral reef benthic community productivity (Leichter et al. 2003). Spatial heterogeneity in water flow can also drive benthic zonation, favoring algal dominance in more benign, low-flow environments (McClanahan & Karnauskas 2011). In addition, spatial gradients in wave forcing can drive benthic community patterning and species zonation (Bradbury & Young 1981, Dollar 1982, Franklin et al. 2013, Williams et al. 2013). For example, high wave forcing can reduce overall coral cover and favor wave-tolerant morphologies, such as encrusting corals (Dollar 1982, Storlazzi et al. 2005, Madin et al. 2006) and may shift the entire benthic community to a dominance by low-lying algal species, such as turf algae and crustose coralline algae (CCA) (Williams et al. 2013).

On many coral reefs today, natural biophysical relationships are confounded by the effects of local human impacts (Sandin et al. 2008, Williams et al. in press). Human activities such as urbanization, coastal development, and overfishing of herbivorous fishes can increase sedimentation, lead to nutrient enrichment of coastal environments, and reduce the top-down control of seaweeds (Hughes 1994, McCook 1999, Fabricius et al. 2005, Wooldridge 2009). Ultimately, the combination of these effects can tip the balance in favor of fleshy benthic regimes, for example dominance by seaweeds and turf algae. In contrast, coral reefs free from local human impacts tend to be characterized by calcifying (reef-building) benthic regimes where hard corals and crustose coralline algae dominate (Sandin et al. 2008, Vroom et al. 2010, Williams et al. 2013). Because human impacts are so ubiquitous, it is challenging to distinguish between natural and human-induced shifts in competing benthic regimes (Williams et al. in press). In order to prevent or even reverse the loss of ecosystem services that coral reefs provide (e.g. fisheries, coastal protection, and tourism), we need a better understanding of the processes that drive dramatic shifts in coral reef community regimes and their associated ecological thresholds or 'tipping points' (McClanahan et al. 2011). To date, focus has been on identifying thresholds for benthic community regimes associated with gradients in fish biomass, pollution, urban development, and variations in human population density (McClanahan et al. 2011, D'agata et al. 2014, Jouffray et al. 2015). There are currently a limited number of examples clearly identifying thresholds associated with gradients in natural physical drivers on coral reefs (Madin 2005, Madin & Connolly 2006).

In this study, we explicitly tested whether coral reef benthic regimes exhibit non-linear, threshold-type responses to natural gradients in physical drivers. We used Palmyra Atoll — a remote, steep-sided oceanic atoll that has been exposed to minimal human influence over the last half century — as a case study system to examine for these effects in the absence of confounding local human impacts (see Fig. 1). We quantified intra-atoll gradients in physical drivers (waves, currents, and temperature) collected from 6 equally spaced locations around the perimeter of Palmyra over a year-long period. *In situ* wave data were used to ground-truth a global wave model to set boundary conditions for a coupled hydrodynamic model, enabling a high spatial resolution assessment of wave-driven stress on the benthos. Bathymetric data collected via multibeam surveys of Palmyra were used to quantify geomorphic complexity and as input for the hydrodynamic model. We quantified spatial patterning in coral reef benthic communities by analyzing thousands of digital images collected via towed divers in a complete circumnavigation of Palmyra's forereef habitat (~40 km). Specifically, we quantified changes in the percent cover of 5 benthic functional groups (hard coral, CCA, macroalgae, turf algae, and soft coral) as well as relative shifts in the 3 most dominant coral morphologies (encrusting, plating, and branching). We then related these shifts in benthic community structure to coupled changes in

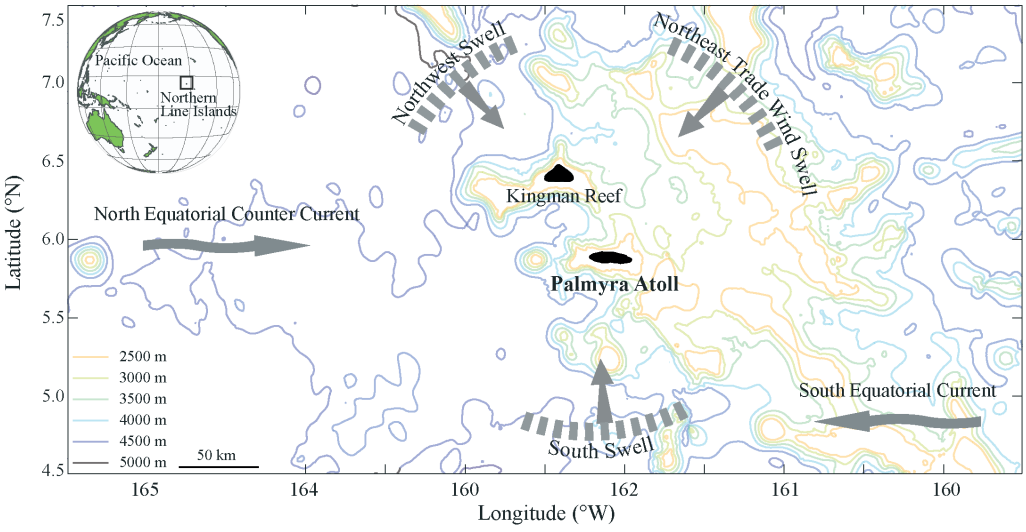

Fig. 1. US-owned atolls in the northern Line Islands of the central Pacific (inset globe), highlighting the dominant wave regimes, regional currents, and seafloor bathymetry

physical drivers (wave forcing and geomorphic complexity) using boosted regression trees (BRT), a stochastic predictive modeling technique that allows for non-linear relationships in the response variables (Elith et al. 2008). In summary, we found benthic communities at Palmyra to exhibit non-linear, threshold-type responses to gradients in natural physical drivers, such as wave forcing, with shifts in the relative dominance of key benthic competitors (e.g. turf algae vs. CCA) occurring at clearly identifiable tipping points.

MATERIALS AND METHODS

Study site

Palmyra Atoll is a remote, oceanic atoll in the northern Line Islands in the equatorial Pacific, approximately 1600 km south of Hawai'i (Fig. 1). Palmyra's physical environment is relatively temperate compared to most other islands and atolls in the Pacific (Gove et al. 2013), with average seasonal ocean surface temperatures ranging from 27.30 to 28.76°C. Regional currents are influenced by the North Equatorial Counter Current (Fig. 1), an eastward flowing current that seasonally migrates in both strength and location (Tomczak & Godfrey 1994). Known historical disturbance is minimal at Palmyra. Reported coral bleaching (Williams et al. 2010) and coral disease (Williams et al. 2011a) has been limited, while reported hurricane impact has been absent owing to Palmyra's proximity to the equator and associated weak Coriolis force, a prerequisite for tropical cyclone formation (Chang et al. 2003). Palmyra has also experienced limited human influence, receiving official protection as a US National Wildlife Refuge in 2001 and further protection as a Pacific Remote Islands Marine National Monument in 2009. Palmyra's coral reef ecosystem therefore represents a biodiversity hotspot in the central Pacific (Williams et al. 2008, Maragos & Williams 2011), characterized by a high cover of calcifying benthic organisms (Williams et al. 2013) and high predatory fish biomass (DeMartini et al. 2008, Sandin et al. 2008).

Oceanographic and geomorphological data

Oceanographic moorings were deployed at 6 fore-reef locations roughly equally spaced around Palmyra (Fig. 2). All moorings were affixed to the benthos at ~20 m. Temperature data were collected using a Sea Bird Electronics (SBE) 37 (accuracy of 0.002°C). Profiling current and spectral wave data were collected using a 1 MHz Nortek Aquadopp acoustic Doppler profiler (ADP) (Table 1).

Currents

Variance ellipses were calculated for near-bottom currents at the 4 moorings in which current data were collected (Northwest, Northeast, Southeast, Southwest). Variance ellipses represent the magnitude (± 1 SD from mean current flow) and orientation of water flow based on the time period of data collection. Power spectral density was calculated to identify the principle frequencies of time-dependent variability for near-bottom currents at each mooring.

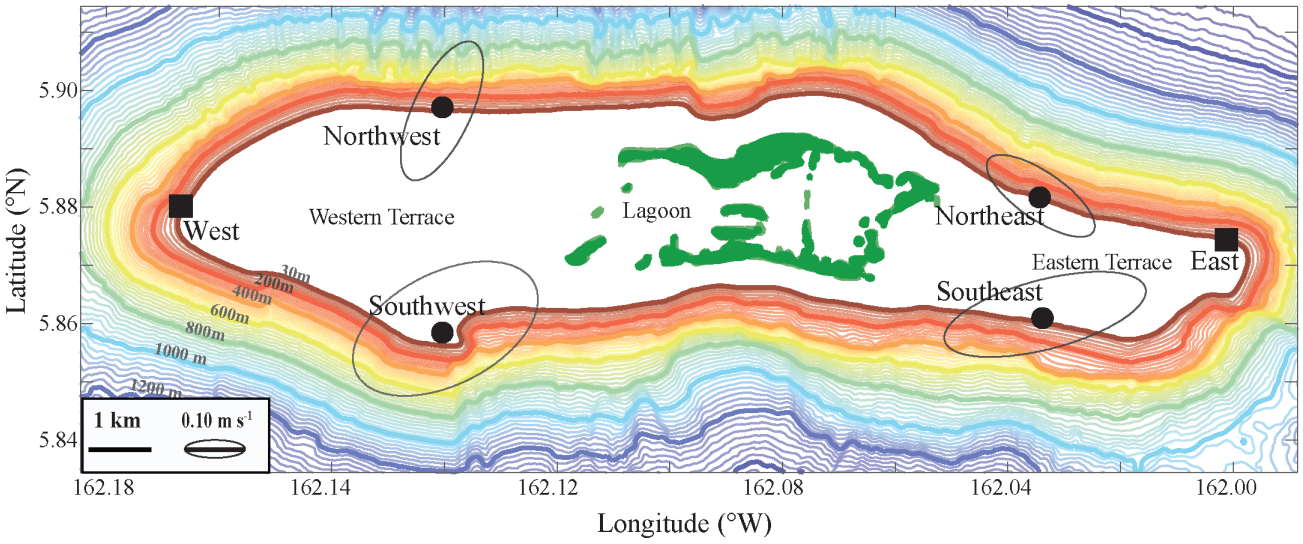

Fig. 2. Palmyra Atoll, showing the 6 mooring locations where oceanographic time series data were collected along the ~20 m isobath. ●: moorings where profiling currents, waves and temperature data were collected; ■: moorings where only temperature data were collected. Current variance ellipses represent the magnitude (± 1 SD from mean current flow) and orientation of near-bottom currents. The scale bar for current magnitude is also given (0.10 m s^{-1})

Table 1. Physical data types used in the analysis, including location, parameters measured, depth, date range, data source, and other relevant information (e.g. sampling interval). Moored-instrument dataset lengths varied due to battery and/or instrument failure. See Fig. 2 for locations of *in situ* oceanographic moorings. NA: not applicable; BSS: bed shear strength (maximum, mean, and range)

Location	Parameter	Depth (m)	Date range	Instrument/ Data source	Sampling interval/ Resolution
***In situ* oceanographic data**					
West	Temperature	19.2	16 Apr 2010–03 May 2011	SBE37	2.5 min
Northwest	Temperature	21.5	16 Apr 2010–03 May 2011	SBE37	2.5 min
	Currents		08 Apr 2010–29 July 2010	Nortek 1MHz Aquadopp	1 min native/20 min average
	Waves		08 Apr 2010–29 July 2010		20 min burst every 3 h
Northeast	Temperature	19.8	16 Apr 2010–03 May 2011	SBE37	2.5 min
	Currents		09 Apr 2010–15 Oct 2010	Nortek 1MHz Aquadopp	1 min native/20 min average
	Waves		09 Apr 2010–15 Oct 2010		20 min burst every 3 h
East	Temperature	21	16 Apr 2010–03 May 2011	SBE37	2.5 min
Southeast	Temperature	18.9	16 Apr 2010–03 May 2011	SBE37	2.5 min
	Currents		09 Apr 2010–29 Dec 2010	Nortek 1MHz Aquadopp	1 min raw/20 min average
	Waves		09 Apr 2010–29 Dec 2010		20 min burst every 3 h
Southwest	Temperature	19.8	16 Apr 2010–03 May 2011	SBE37	2.5 min
	Currents		08 Apr 2010–20 Dec 2010	Nortek 1MHz Aquadopp	1 min raw/20 min average
	Waves		08 Apr 2010–20 Dec 2010		20 min burst every 3 h
Gridded data					
Atoll wide	Bathymetry	0–3000	NA	Ship-based multibeam and Ikonos imagery	5 m resolution
Forereef	Slope Slope of slope BPI	15–20	NA	ArcGIS 10.1	5 m resolution
Modeled data					
Atoll wide	Wave height Peak period Peak direction	NA	1 Jan 2005–12 Apr 2010	Wave Watch III	1° resolution
Forereef	BSS_{max}, BSS_{mean}, BSS_{range}	15–20	1 Jan 2005–12 Apr 2010	Delft3D	50 m resolution

Temperature

Temperature data were also analyzed to assess the principle frequencies of time-dependent variability (i.e. power spectral density) observed at each mooring location. We further analyzed the temperature data to quantify the site-specific characteristics in temperature drops observed in each of the temperature records. Following Sevadjian et al. (2012), we quantified the number of temperature drops based on the following equations:

$$\frac{T_{i+n} - T_i}{t_{i+n} - t_i} \leq \frac{-0.3°C}{240\,\text{min}} \quad (1)$$

$$T_{i+n} - T_i \leq -0.3°C \quad (2)$$

where T is temperature (°C), t is time (min), and for the i^{th} temperature measurement, n = 1, 2, 3, etc. To be quantified as a 'temperature drop', the following criteria had to be satisfied: (1) the rate of change of T with respect to t must maintain a gradient of ≤−0.3°C per 240 min, and (2) the total decrease in temperature (ΔT) must be ≤−0.3°C. The duration of each temperature drop was calculated as the time from the initial decrease in temperature to the minimum temperature. A temperature drop concluded when temperature returned to 0.5 × ΔT. Analysis of temperature drops was constrained to the temporal extent of tidal return periods (≤12.4 h).

Wave forcing

We incorporated the 3-h output of mean significant wave height (H_s), peak period (t_p), and peak direction d_p) from Wavewatch III (WWIII; http://polar.ncep.noaa.gov/waves). WWIII performance was assessed at Palmyra by comparing the model output with *in situ* wave data collected from each wave sensor (Fig. 1). Wave power (E_f) in kilowatts per meter (kW m^{-1}) was calculated for both data sets based on the following equation:

$$E_f = \frac{\rho g^2}{64\pi} H_s^2 t_p / 1000 \quad (3)$$

where ρ is the density of seawater (1024 kg m^{-3}) and g is the acceleration of gravity (9.8 m s^{-2}). Wave power combines H_s and t_p and provided a more representative metric of the most powerful wave events than either H_s or t_p alone. The 15 largest wave events (event = maximum daily wave power) from each sensor were identified, and differences between WWIII and *in situ* wave parameters were calculated for each event. The mean difference in H_s, t_p, and d_p was then used as a correction factor for peak wave events in the WWIII data record. Comparisons between data sets were constrained to incident (i.e. perpendicular) swell angles at each sensor, minimizing shadowing and other wave-bathymetry interactions (e.g. refraction) that would bias the comparisons.

To provide a high-resolution, nearshore spatial assessment of wave forcing at Palmyra, we incorporated a coupled hydrodynamic model developed by Delft Hydraulics (Delft3D; http://oss.deltares.nl/web/delft3d). A total of 3 model runs were performed, one for each wave regime (Fig. 1): northwest swell (H_s = 3.4 m, t_p = 16.9 s, d_p = 330°), northeast trade wind swell (H_s = 4 m, t_p = 10 s, d_p = 41°), and south swell (H_s = 2.8 m, t_p = 14 s, d_p = 172°). Modeled wave conditions corresponded to a wave regime-specific annual maximum H_s, t_p, and d_p, calculated from the corrected WWIII data set by averaging the largest annual events for each wave regime over the time period encompassing the ecological surveys described below (January 2005–April 2010). Results from the 3 model runs were combined to calculate an annual average maximum, mean and range in wave forcing at Palmyra. A full description of Delft3D is given by Lesser et al. (2004), with detailed information on the waves portion of the model given by Booij et al. (1999). See 'Supplemental methods' (in the Supplement at www.int-res.com/articles/suppl/m522p033_supp.pdf) for more detail relating to our wave model.

Hydrodynamic stress induced by waves and currents near the benthic-water interface was used here to represent wave forcing at Palmyra. Bed shear stress (BSS) was chosen over more traditional surface-level wave metrics (e.g. wave height) because it specifically quantifies forcing at the depth of benthic organisms (15–20 m in this study) and drives benthic community structure on wave-dominated reefs (Storlazzi et al. 2005, Williams et al. 2013).

Geomorphological data

Multibeam bathymetric data were collected during NOAA's Reef Assessment and Monitoring Program (RAMP) survey of Palmyra in 2006 and were provided by the Pacific Islands Benthic Habitat Mapping Center (www.soest.hawaii.edu/pibhmc). Multibeam data collection was incomplete from 0–25 m depth due to navigational hazards associated with shallow reef environments. We therefore used IKONOS

satellite imagery to create estimated depths and fill bathymetric gaps that existed within this depth range (Lyzenga 1985) (see 'Supplemental methods'). To quantify the structural habitat complexity of the underlying habitat at Palmyra, 3 geomorphic metrics were derived from the 5 m gridded bathymetry data: slope, the rate of change of slope (i.e. slope of slope), and bathymetric position index (BPI). Slope and slope of slope (calculated in degrees) were derived from the bathymetric grids using the slope function in the ArcGIS v10.1 Spatial Analyst toolbox, where the raster cell values represented the maximum rate of maximum slope change between neighboring cells. BPI represents a location's elevation relative to overall surrounding seascape (Lundblad et al. 2006). A negative BPI value indicates a location lower than neighboring locations (e.g. sand channel, groove), a positive indicates a location higher than neighboring locations (e.g. pinnacle top), and near-zero values indicate flat areas. BPI was calculated with a search radius of 10 cells (i.e. 50 m) using the Bathymetric Terrain Modeler application in ArcGIS v10.1 (Wright et al. 2012).

Benthic community surveys

Benthic community data were collected via towed-diver surveys of Palmyra in 2006, 2008, and 2010. Towed-diver surveys incorporated divers on SCUBA that maneuver instrumented boards ~1 m above the benthos while being towed behind a small boat at ~3 km h^{-1}. The board is equipped with a high-resolution digital camera (Canon EOS 10-D/50-D), strobes to illuminate the bottom substrate, a pair of red lasers at a known distance apart to quantify area per frame, and a temperature-depth recorder. Position information was recorded by an onboard Global Positioning System (GPS), to which a layback model was applied to accurately georeference each individual benthic photograph. Benthic photographs were obtained at 15 s intervals for the duration of each tow. A detailed description of the towed-diver technique is given by Kenyon et al. (2006).

Benthic photographs from the forereef habitat (15–20 m only) were analyzed for percent cover of 5 benthic functional groups (hard coral, CCA, macroalgae, turf algae, and soft coral) using Coral Point Count with Excel Extensions (Kohler & Gill 2006). Within the hard coral functional group, the percent cover of 5 morphological subcategories (encrusting, branching, plating, massive, and free-living) were also quantified. Only the 3 most dominant (encrusting, plating, and branching) were investigated further in this study. Wave and geomorphological information was obtained for each individual photograph using the Sample routine in the ArcGIS v10.1 Spatial Analyst toolbox. In total, 3237 photographs were incorporated into the analyses, with a mean (± SD) distance between consecutive images of 11.7 (± 30) m.

Ecological statistical analyses

Benthic data were averaged over 50 m linear segments in a continuous fashion around the circumference of Palmyra's forereef. To identify and account for spatial autocorrelation between the linear segments, 2 techniques were employed: empirical semivariance (Meisel & Turner 1998) and lacunarity (Mandelbrot 1983, Plotnick et al. 1993). Empirical semivariance calculations were completed using the *vgm* function in the *gstat* package (Pebesma 2004) linked to a custom coded function in R v2.15.1 (R Development Core Team; www.r-project.org). Visual assessment of semivariance plotted against distance indicated that 500 m was the minimum distance required between linear segments to avoid spatial autocorrelation and achieve true data independence. We further employed lacunarity indices to avoid averaging over distances that were either too large (i.e. averaging across true signals in the data) or too small (i.e. incorporating noise into the signal). As with empirical semivariance, lacunarity indices indicated that 500 m was the optimal spatial scale at which to model the semi-continuous benthic data in order to account and adjust for spatial autocorrelation (see 'Supplemental methods' for more detailed information on these spatial analyses).

Boosted regression trees (BRTs) were used to examine the relationship between the benthic response variables and physical predictors (Elith et al. 2008). BRTs were constructed using the routines *gbm* (Ridgeway 2012) and *gbm.step* (Elith et al. 2008) in R. Benthic percent cover values were arcsine transformed to achieve normality and modeled using a Gaussian distribution. We used 10-fold cross validation for model development and validation and cross validation deviance (CVD) to assess model performance. Overall percent deviance explained by each model was also quantified to provide a more widely understood metric of model performance. The optimal combination of tree complexity (*tc*, number of nodes in the tree), learning rate (*lr*, contribution of each tree as it is added to the model), and the bag-fraction (*bf*, proportion of data to be selected at each

step of the model) was identified using a customized loop routine in R (Richards et al. 2012). The parameter combination that produced the lowest CVD, while maintaining ≥1000 fitted trees, was used to fit the final model. The relative importance of each predictor variable was quantified based on the number of times it was selected for splitting, weighted by the squared improvement to the model as a result of each split and averaged over all trees (Friedman & Meulman 2003, Elith et al. 2008). Partial dependency plots were used to interpret the relationship between each predictor and the final fitted function of the model in a conditional manner. To quantify interaction effects between predictors within each model (departure from a purely additive effect), we used the function *gbm.interactions* (Elith et al. 2008).

RESULTS

Gradients in physical drivers

Near-reef currents

Variance ellipses representing the magnitude and orientation of near-reef current measurements indicate that water flow was predominantly influenced by local bathymetry and geographic location around Palmyra (Fig. 2). At the Northeast mooring, located proximate to shallow and emergent reef with generally parallel isobaths offshore, current was comparatively weak and predominantly along isobaths (i.e. along-shelf). Conversely, currents at the Southeast mooring were stronger and less aligned with nearshore bathymetry, likely owing to the sensor's location along the Eastern Terrace, a broad, open area of reef with generally consistent depth (~10–15 m) and no emergent obstructions (Fig. 2). Current at the Southwest mooring had both a strong along-shelf and cross-shelf (perpendicular to isobaths) component. The bathymetric outcropping that extends ~500 m from the east–west orientation of the atoll presumably drives the mixed directional flow patterns in this area. Currents at the Northwest mooring were predominantly cross-shelf, perhaps due to deep offshore channels funneling water up-slope at this location (Fig. 2). Current oscillations at all moorings varied primarily at tidal frequencies, with the diurnal (K_1; 23.934 h per cycle) and semi-diurnal (M_2; 12.421 h per cycle) tides as the principal tidal constituents (Fig. S1 in the Supplement at www.int-res.com/articles/suppl/m522p033_supp.pdf). The semi-diurnal tide was the strongest influence on current oscillations at the Northwest, Northeast, and Southeast moorings, whereas the diurnal and semi-diurnal tides were equally influential at the Southwest mooring.

Subsurface temperature

Reef-level temperatures recorded from 6 equally spaced locations over a year-long time period ranged from 24.87 ± 0.17°C (mean ± SD) to 28.72 ± 0.02°C (Fig. 3). Seasonal forcing was nearly absent across sites; however, shorter-term fluctuations were dominant in all temperature records, with high-frequency fluctuations exhibiting unique site-specific characteristics. Large-amplitude temperature decreases were recorded on intra-seasonal time scales, often persisting for multiple days to weeks. For example, 2 prominent temperature decreases of 2.0–4.0°C were observed in October and November, driving strong temperature changes at all moorings lasting for ~3–4 wk. Superimposed over intra-seasonal variability were high-frequency temperature drops of 0.3–1.8°C occurring multiple times daily and lasting for minutes to hours (Fig. 3). Many were solitary, knife-like temperature drops with a subsequent and equally rapid recovery to ambient temperatures. However, temperature changes also occurred as a series of 3–10 discrete, successional temperature drops of varying magnitude; a sharp decrease followed by gradual recovery; a gradual decrease superimposed with saw-toothed oscillations; and a step-like decrease characterized by a sharp temperature drop that persisted for several hours before sharply returning to pre-event temperatures (Fig. 3B).

Site-specific temperature characteristics differed spatially around Palmyra (Fig. 3B and Table S1 in the Supplement). For example, the greatest number of temperature drops (339) occurred at the East mooring. In contrast, 102 and 109 temperature drops were recorded at the Northwest and Southwest moorings, respectively; a 3.11- to 3.33-fold decrease from the East mooring (Table S1). The duration of temperature drops was also spatially variable. Nearly half (48%) of the temperature drops recorded at the Southeast mooring lasted for 120–720 min, while approximately the same proportion (43–52%) at all other locations occurred over shorter time scales (30–120 min; Table S1). In addition, differences in the principle frequencies of temperature oscillations at each mooring were apparent (Fig. S2 in the Supplement). Semi-diurnal variability, for example, was a prominent frequency of oscillation at most

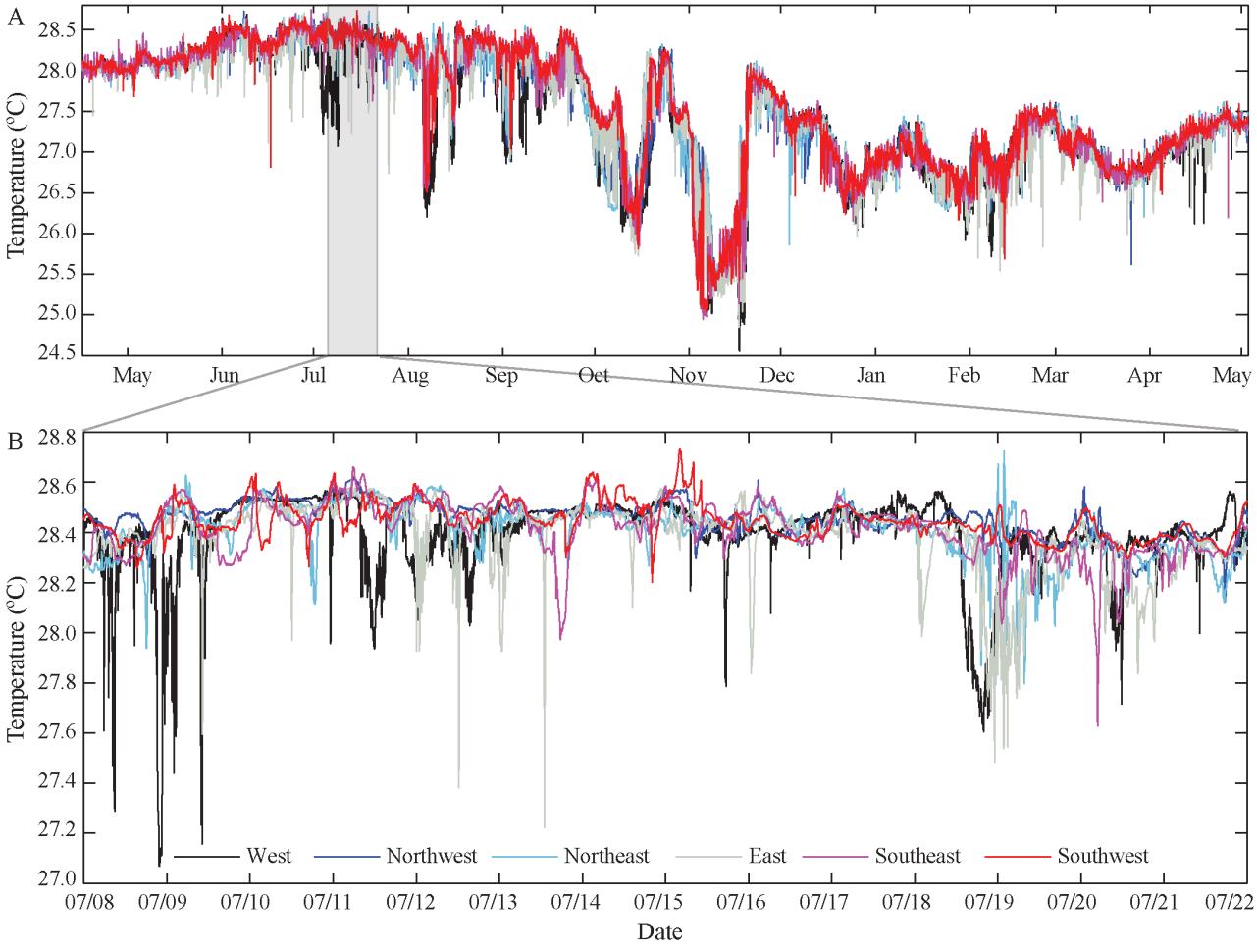

Fig. 3. (A) *In situ* time series data of temperature from 6 mooring locations deployed at ~20 m depth from April 2010 to May 2011. (B) Two-week expansion of temperature data highlighting the high-frequency temperature drops observed at all locations. Legend in (B) corresponds to both panels. See Fig. 2 for indvidual mooring locations

locations, with the exception of the Southwest mooring (Fig. S2), an unexpected result given the strength of the semi-diurnal tide observed in current fluctuations at the same location (Fig. S1).

Waves and bed shear stress

Consistent features emerged from the combined wave model results (i.e. northwest swell, northeast trade wind swell, and south swell; Fig. 1). First, the central lagoon–reef complex partially blocks incoming waves from reaching the southern portion of the atoll, creating a lee from the largest wave source (Fig. 4). Second, wave forcing was markedly enhanced over the emergent reef encircling the lagoon–reef complex, particularly with respect to maximum bed shear stress (BSS_{max}; Fig. 4C). Strong dissipation occurs over the emergent reef due to increased bed shear stress associated with breaking waves. Third, wave forcing was enhanced over portions of the Western and Eastern Terrace where multiple wave regimes converge. Intra-atoll gradients in wave forcing were also observed in the depth-constrained (15–20 m) and spatially averaged (50 m linear segments) model results (Fig. 5A,B). In general, mean bed shear stress (BSS_{mean}) was greatest along the southwest, west, and northwest sections of the atoll, with BSS_{max} peaking (142 N m^{-2}) between the southwest and west (Fig. 5B). This geographic area exposed to the greatest BSS_{max} was also characterized by the largest range in bed shear stress (BSS_{range} = 119 N m^{-2}), indicating variable annual wave forcing. From the northwest towards the north and northeast, bed shear stress declined by ~50 % before increasing proximate to the eastern tip of the atoll. Wave forcing near the southeast and south sections was comparatively low (BSS_{max} = 10–20 N m^{-2}, BSS_{mean} = 1–10 N m^{-2}, BSS_{range} = 10–20 N m^{-2}).

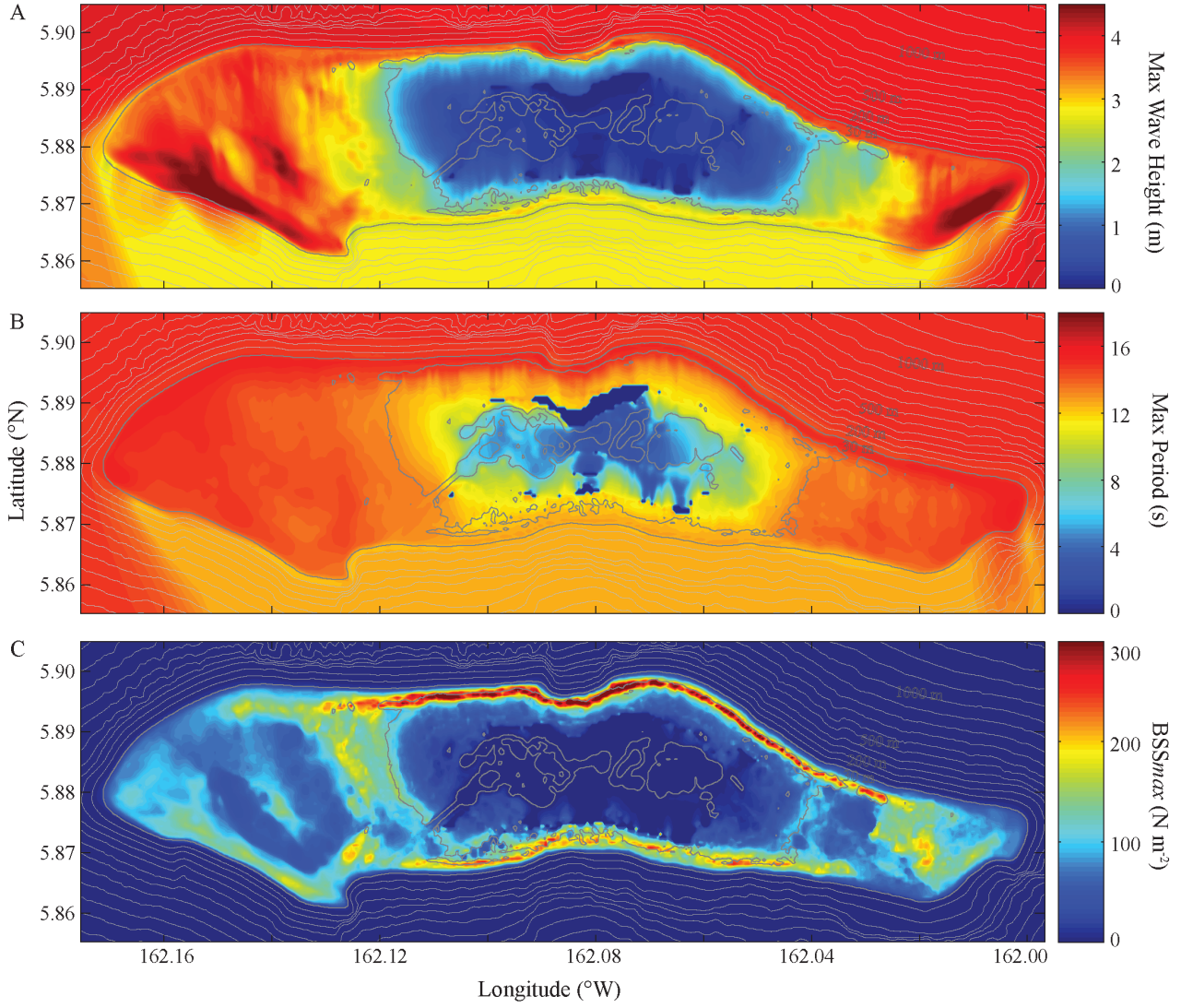

Fig. 4. Hydrodynamic wave model results representing the maximum values of (A) significant wave height, (B) wave period, and (C) bed shear stress (BSS_{max}) at Palmyra Atoll. Results represent the maximum of each grid cell from the combined hydrodynamic model runs for each swell regime (i.e. northwest swell, northeast trade wind swell, and south swell) at Palmyra Atoll (see Fig. 1)

Geomorphology

Palmyra's forereef habitat was generally characterized by a slope range of 10–15°, although steeper slopes (25–30°) were consistently observed along the southern forereef (Fig. 5C). The southern forereef also had the greatest rate of change in slope (50–60°), while other portions of the forereef exhibited enhanced variability at finer spatial scales, with proximate segments (i.e. separated by 50 m) regularly characterized by a 10–20° rate of slope change, with some segments differing by 45°. Differences in bathymetric position index (BPI) indicated within-atoll variability in relative reef elevation, which was often closely negatively related to slope of slope (Fig. 5D).

Benthic community spatial patterns

Palmyra's coral reef benthic communities were dominated by hard coral (atoll-wide mean cover = 27.3%) and CCA (21.8%). The remaining space was occupied by turf algae (16.5%), soft coral (14.5%), and erect macroalgae (10.8%). At smaller spatial scales, benthic functional groups exhibited unique spatial patterning (Fig. 5E–I). Hard coral cover was variable at both large and small spatial scales (Fig. 5E). Relatively high coral cover (>50%) was observed in the west, northeast, southeast, and southwest sections of the forereef; however, 10–20% changes in coral cover also occurred within relatively small distances (<250 m). Conversely, patterns of macroalgae cover were far less spatially complex (Fig. 5G). Nearly all macroalgae

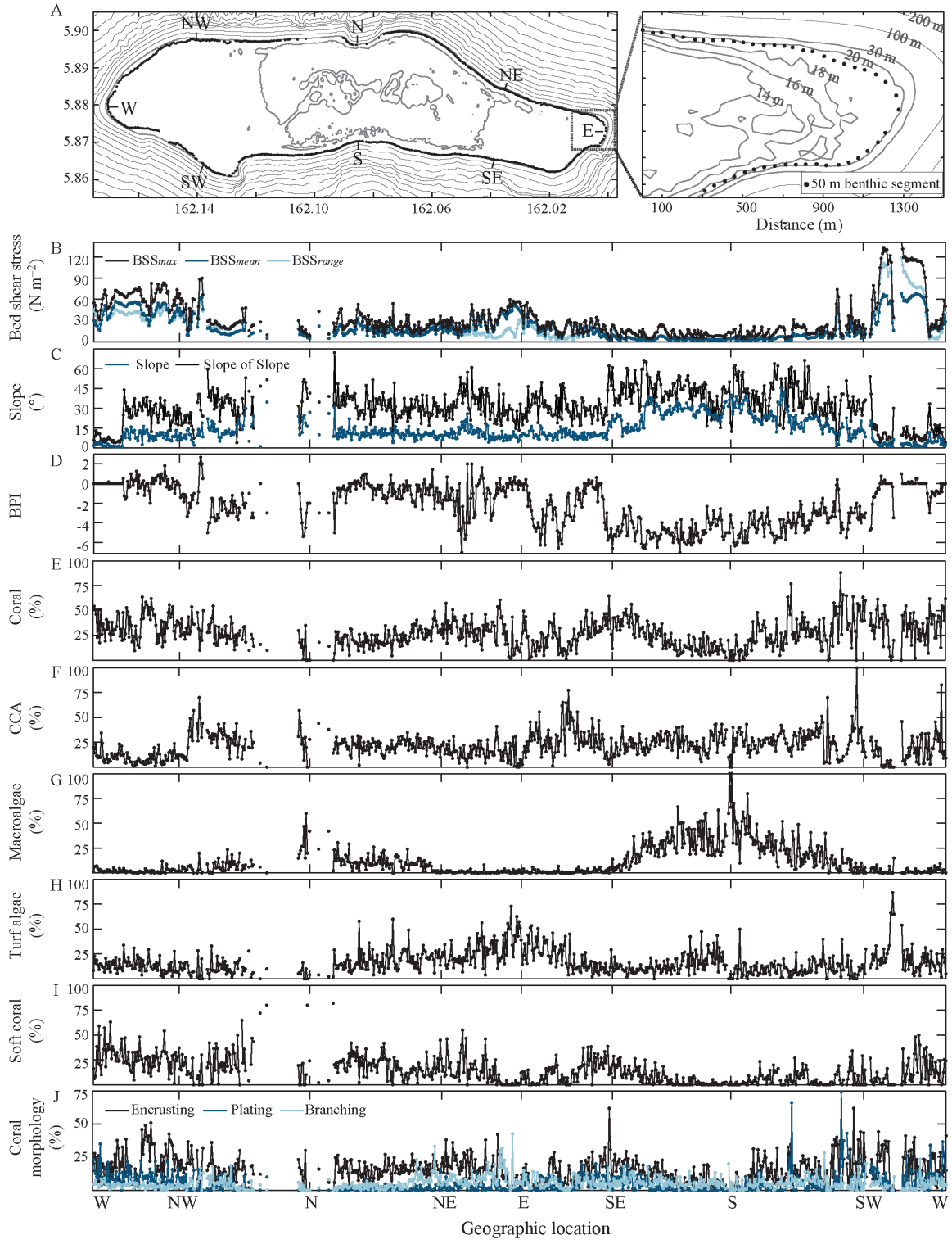

Fig. 5. (A) Bathymetric map of Palmyra Atoll (left) with an expanded section (right) showing depth-constrained (15–20 m) and spatially averaged 50 m benthic segments collected via towed-diver surveys (black filled circles). (B–J) Corresponding wave, geomorphology, and coral reef benthic community data for each 50 m segment. Note the *x*-axis ('Geographic location') corresponds to (A, top left), showing all data in a clockwise fashion from left to right, starting at the western tip of the atoll (W) and moving northwest (NW), north (N), northeast (NE), east (E), southeast (SE), south (S), southwest (SW), and ending back at the western tip. (B) Bed shear stress (maximum, mean, and range), (C) slope (and slope of slope), (D) bathymetric position index (BPI), and percent cover of (E) hard coral, (F) crustose coralline algae (CCA), (G) macroalgae, (H) turf algae, (I) soft coral, (J) variations in the 3 most dominant hard coral morphologies (encrusting, plating, branching)

Table 2. Results from boosted regression tree (BRT) analyses, including optimal parameter settings, predictive performance, and relative influence of physical drivers on variations in the percent cover of 5 dominant benthic functional groups: hard coral, crustose coralline algae (CCA), macroalgae, turf algae, and soft coral; and 3 dominant coral morphologies: encrusting, plating, and branching. BSS: bed shear strength (maximum, mean, and range)

	Functional group					Coral morphology		
	Hard coral	CCA	Macro-algae	Turf algae	Soft coral	Encrust-ing	Plating	Branch-ing
Model parameters								
Tree complexity	4	4	4	2	3	3	4	2
Learning rate	0.001	0.001	0.0001	0.001	0.001	0.0001	0.001	0.001
Bag fraction	0.8	0.8	0.7	0.7	0.8	0.8	0.8	0.7
Number of trees	2550	1450	26750	3350	1350	15400	1200	10650
Mean total deviance	0.00910	0.00784	0.01532	0.00684	0.00974	0.00680	0.00264	0.00110
CV deviance (CVD)	0.00812	0.00239	0.00312	0.00322	0.00466	0.00301	0.00174	0.00073
CVD SE	0.00100	0.00122	0.00087	0.00082	0.00071	0.00110	0.00131	0.00081
Deviance explained (%)	10.8	69.6	79.6	52.9	52.2	55.7	34.1	33.6
Relative influence of predictors (%)								
BSS_{max}	9.66	9.30	18.02	2.72	7.88	7.77	17.37	10.00
BSS_{mean}	6.29	46.14	16.11	34.94	6.61	4.30	3.32	7.55
BSS_{range}	33.90	3.11	2.48	21.56	49.49	46.56	38.46	41.87
Slope	24.29	11.13	58.04	17.27	16.58	12.57	8.36	18.13
Slope of slope	12.31	20.31	2.48	5.39	4.94	8.96	27.51	15.68
BPI	13.55	10.01	2.88	18.13	14.50	19.85	4.98	6.79

were observed in 2 distinct regions: a small section to the north (250 m) and a much larger section to the south (~6 km), where cover was regularly >30% and even as high as 100%. Approximately half (52%) of all other areas surveyed along the forereef were characterized by ≤5% macroalgae cover. CCA, turf algae, and soft coral were also spatially heterogeneous, varying from a minimum (<5%) to a majority (>50%) of the benthic substrate (Fig. 5F,H,I).

The 3 most dominant hard coral morphologies (encrusting, plating, and branching) also exhibited complex within-atoll spatial patterning (Fig. 5J). Encrusting corals were by far the most abundant, accounting for 25–50% of overall hard coral cover. However, shifts in the relative dominance of the 3 morphologies occurred in particular locations. For example, to the west of the atoll, overall hard coral cover equaled 40%, with encrusting and plating morphologies contributing equally. To the east, branching corals dominated a small stretch of reef (~250 m), and to the south of the atoll plating corals dominated, reaching 65–75% cover (Fig. 5J).

Biophysical relationships and thresholds to physical drivers

Overall, hard coral cover was positively related to the range in bed shear stress (BSS_{range}) and negatively related to slope. Hard coral cover was weakly positively related at lower BPI values and negatively related at higher BPI values (Table 2, Fig. 6A). However, because total deviance explained for hard coral cover was low (10.8%), these relationships should be interpreted with caution. Interestingly, predictive performance improved 3–5 fold when hard coral morphological categories were modeled as the response variables (Table 2). The relative dominance of encrusting corals increased dramatically above a threshold BSS_{range} of 10 N m^{-2} (Table 2, Fig. 6F); their relative abundance also peaked at a BPI level of −3, but decreased with increasing reef slope. The best-fit model explained 55.7% of the total deviance in encrusting coral cover (Table 2). Similarly, the relative dominance of plating corals was also positively related to BSS_{range}; however the threshold for a dramatic increase in their relative dominance was higher at a BSS_{range} of ~23 N m^{-2} (Table 2, Fig. 6G). The relative dominance of plating corals was also negatively related to the rate of change of slope (slope of slope) and positively related to BSS_{max}, showing a peak in relative dominance above a threshold ~50 N m^{-2}. The best-fit model explained 34.1% of the total deviance in plating coral cover (Table 2). In contrast to encrusting and plating corals, the relative dominance of branching corals was negatively related to BSS_{range}, with a dramatic decline occurring at a threshold of ~20 N m^{-2} (Table 2, Fig. 6H). The cover of branching corals also declined sharply above a threshold reef slope of 10°, although it increased where slope of

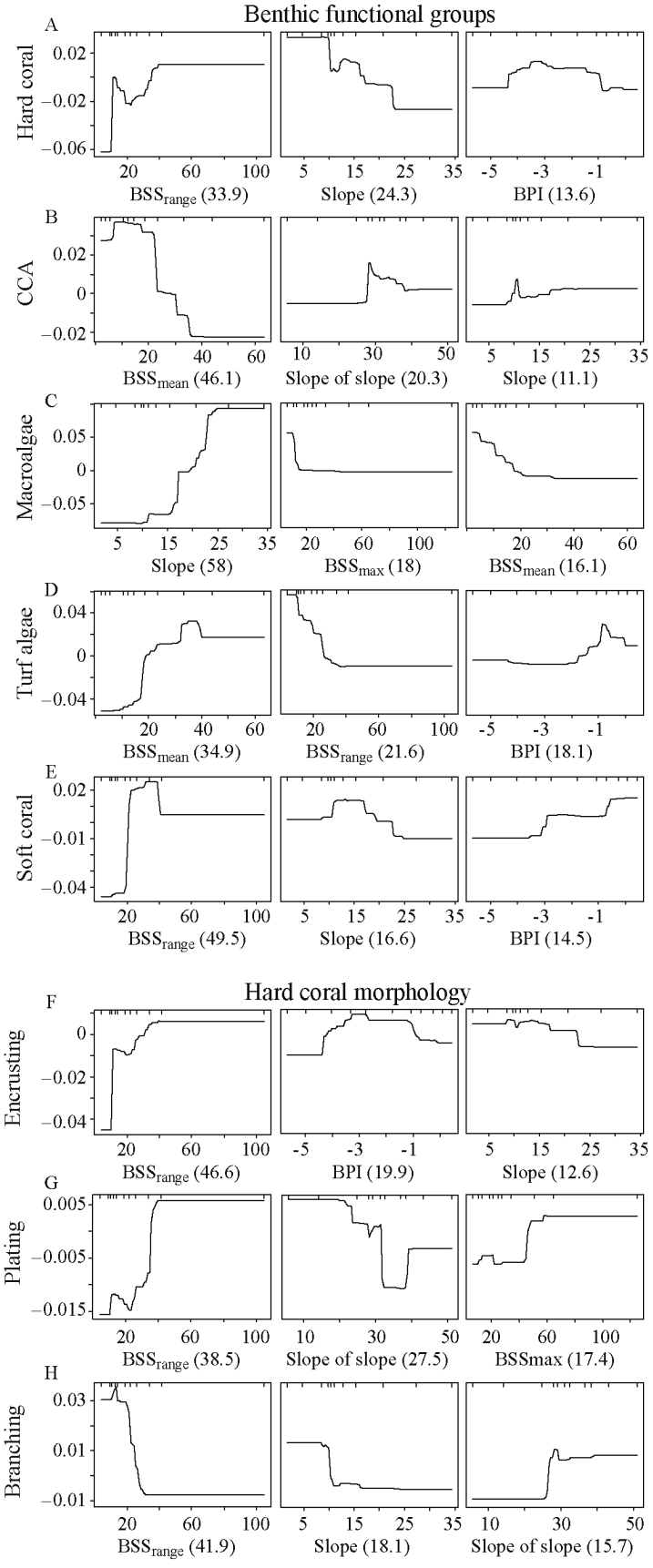

Fig. 6. Partial dependency response plots from boosted regression tree analyses for the 3 most influential predictors of variations in the percent cover of 5 dominant benthic functional groups: (A) hard coral, (B) crustose coralline algae (CCA), (C) macroalgae, (D) turf algae, and (E) soft coral; and 3 dominant hard coral morphologies: (F) encrusting, (G) plating, and (H) branching. Relative influence of each variable is given in parentheses after the *x*-axis label. The *y*-axes are on logit scale and are centered to have zero mean over the data distribution. Tick marks along the inside top of each subpanel indicate the distribution of the replication for that variable (e.g. hard coral) across the corresponding predictor (e.g. slope). BPI: bathymetric position index; BSS_{max}, BSS_{mean}, BSS_{range}: bed shear stress maximum, mean, and range, respectively

slope exceeded ~28°. The best-fit model explained 33.6% of the total deviance in branching coral cover (Table 2).

Similarly to hard coral communities, the relative dominance of other benthic functional groups displayed evidence of non-linear threshold responses to gradients in key physical drivers. The relative dominance of CCA decreased dramatically at a threshold BSS_{mean} of 18 N m^{-2} (Table 2, Fig. 6B); cover also appeared to be positively related to reef slope (both slope and slope of slope). The best-fit model explained 69.6% of the total deviance in CCA cover (Table 2). Coinciding with the sharp decline in CCA cover was a dramatic increase in the relative dominance of fleshy turf algae at the same 18 N m^{-2} BSS_{mean} threshold (Fig. 6D). In contrast to a positive relationship with BSS_{mean}, the relative dominance of turf algae decreased with increasing BSS_{range}, dropping in cover above a threshold of ~10 N m^{-2}. Finally, the relative dominance of turf algae was positively related to BPI, peaking above a value of −1 (Fig. 6D). The best-fit model explained 52.9% of the total deviance in turf algae cover (Table 2). Macroalgae relative dominance was positively related to reef slope and showed a dramatic increase at a threshold slope of ~15° (Table 2, Fig. 6C). Macroalgae cover was also negatively related to BSS_{max}, dropping in cover sharply at a BSS_{max} threshold of 10 N m^{-2}. In addition, macroalgae gradually decreased in relative dominance with increasing BSS_{mean}, but held a steady cover above a BSS_{mean} of 20 N m^{-2} (Fig. 6C). The best-fit model explained 79.6% of the total deviance in macroalgae cover (Table 2). Finally, soft coral relative dominance was positively related to BSS_{range}, with cover increasing dramatically at a threshold of 20 N m^{-2} (Table 2, Fig. 6E). Soft coral cover also peaked at a reef slope between 10 and 17° and was positively related to an increasing BPI. The best-fit model explained 52.2% of the total deviance in soft coral cover (Table 2).

DISCUSSION

Palmyra's benthic community was dominated by calcifying organisms, namely hard coral and CCA, corroborating previous studies (Sandin et al. 2008, Williams et al. 2013). However, at smaller spatial scales (100s of meters to kilometers), benthic community composition exhibited considerable variability, with the percent cover of each benthic functional group (hard coral, CCA, turf algae, erect macroalgae, soft coral) ranging from 0% to >80%. Furthermore, different benthic functional groups displayed different spatial patterning. Macroalgae, for example, was highly spatially clumped, monopolizing (50–100% cover) the benthos over a ~6 km section of the forereef to the south, whereas half of the remaining areas surveyed had ≤5% cover. Hard coral cover, by contrast, was markedly variable, comprising >50% of the benthic community at numerous locations around the atoll.

Coupled biophysical models found wave forcing and geomorphology to be major proximate drivers of benthic regimes around Palmyra, explaining 52–80% of the spatial variability in dominant benthic functional groups. Moreover, distinct biophysical relationships existed among key benthic competitors. For example, CCA and turf algae, both early colonizers and competitors for space on the reef benthos (Grigg 1983, Hughes & Connell 1999), showed a marked shift in relative dominance with increased mean wave forcing. Specifically, a sharp decline in CCA cover was coincident with an increase in turf algae at a mean bed shear stress threshold of 18 N m^{-2}. It is unclear whether competitive exclusion results in a stable turf algae-dominated regime, or if the benthic community is being continually reset to an earlier successional state by repeated disturbance (Hughes & Connell 1999). Nevertheless, our results indicate that a shift to an alternate benthic regime — from a dominance by calcifying organisms, such as CCA, to dominance by fleshy, non-calcifying organisms, such as turf algae — can occur as a consequence of gradients in natural physical drivers even in the absence of local human impacts. Furthermore, we found that shifts in the relative dominance of benthic groups occurs at distinct physical thresholds, showing non-linear responses to wave-driven stress. These findings add to the growing body of evidence that coral reef benthic regimes have clearly identifiable tipping-points in response to an array of both human and natural physical drivers (McClanahan et al. 2011, D'agata et al. 2014, Jouffray et al. 2015, Williams et al. in press).

Macroalgae monopolized the forereef benthic community in a geographic region characterized by steep slopes and low wave forcing. Due to increased vulnerability to physical dislodgement (Engelen et al. 2005), macroalgae are more readily observed where wave forcing is low (Kilar & McLachlan 1989, Page-Albins et al. 2012, Williams et al. in press). Steep slopes may also favor a macroalgal regime by regulating waves. The location at which waves break, and therefore the maximum wave-induced stress imposed on the benthic community, is pushed shoreward in more steeply sloped regions compared to those with more gradual slopes (Raubenheimer & Guza 1996). Therefore, the observed macroalgae regime may persist owing to a reprieve in wave stress mediated by the underlying local reef geomorphology. Alternatively, Williams et al. (2011b) reported comparatively high rates of fine-grained sedimentation where we observed high macroalgal abundance at Palmyra; those authors postulated that this sediment could have originated from nutrient-rich lagoonal waters. Increased sedimentation can inhibit coral recruitment and growth due to smothering and abrasion (Fabricius 2005) and nutrient subsidies can fuel algal growth, tipping the balance in favor of macroalgae over corals (Littler & Littler 1985). Although further research is needed to identify the ultimate underlying driver(s) of the observed macroalgal benthic regime in this region of Palmyra, we postulate that low annual wave forcing in concert with localized increases in sedimentation and lagoon-derived nutrient subsidies may be responsible.

Predictive capacity improved 3- to 5-fold for overall hard coral cover when hard corals were modeled at the morphology level. The susceptibility of corals to hydrodynamic dislodgement is related to the shape of a coral colony (Madin 2005), particularly in more exposed reef habitats such as the forereef (Madin et al. 2006, Madin & Connolly 2006). At Palmyra, variations in the relative dominance of different coral morphologies (i.e. encrusting, plating, and branching) were strongly predicted by variations in wave forcing. Each morphological group exhibited a non-linear, threshold-type response to spatial gradients in the annual range of bed shear stress. Branching corals were found to be the most vulnerable to increased wave-stress, exhibiting a sharp, non-linear decline at a threshold of 20 N m^{-2}. Branching corals have a comparatively higher colony shape factor than encrusting and plating (i.e. tabular) corals, lending to increased vulnerability to wave-induced disturbance (Madin 2005). These results demonstrate that even around a small

atoll, coral assemblages show inherent flexibility and can reorganize in response to physical drivers rather than exhibit wholesale changes in overall cover.

Despite the relatively robust model results presented herein, the inclusion of additional physical drivers characterized at an appropriate spatial scale would presumably increase predictive performance for each of the benthic groups. Specifically, the observed variations in currents and temperature were likely influential drivers of coral reef benthic communities. For example, the high-frequency temperature drops observed in the reef-level temperature measurements have been reported in other coral reef environments and are often attributed to internal waves (Wolanski & Delesalle 1995, Leichter & Miller 1999, Sevadjian et al. 2012). Internal waves, generated by tidal currents interacting with steep bathymetry, can drive localized, rapid fluctuations in water flow, temperature, nutrients, and suspended particles (Wolanski & Delesalle 1995, Leichter et al. 1998). The advection of allochthonous food resources can influence coral reef benthic production (Leichter et al. 2003) and community growth rates (Smith et al. 2004, Roder et al. 2010). Moreover, among-island differences in internal waves have been found to drive intraspecific differences in coral growth, biomass, density of host symbionts, and degree of heterotrophic feeding (Roder et al. 2010, 2011). The present study was unable to resolve the mechanism(s) driving the observed high-frequency temperature fluctuations nor the associated site-specific influence on the benthic community. Future research characterizing temperature and current variability and the associated biological community response at Palmyra would provide important additional insight into naturally coupled biophysical relationships on coral reef ecosystems.

CONCLUSIONS

Due to its remote oceanic environment and absence of direct human impact, Palmyra Atoll provided a unique opportunity to study the independent effects of natural physical drivers on coral reef benthic community regimes. We conclude that dominant coral reef benthic functional groups (hard and soft corals, CCA, turf algae, and macroalgae) show considerable spatial heterogeneity driven largely by intra-atoll gradients in natural physical drivers. In addition, we find that benthic functional groups and different coral morphologies (encrusting, plating, and branching) exhibit threshold-type responses to key physical drivers, leading to non-linear relationships between competing benthic groups. Importantly, our results highlight that shifts in benthic regimes from calcifying (i.e. hard corals and CCA) to non-calcifying regimes (i.e. turf algae) can occur even in the absence of local human impacts. Our study further highlights the innate flexibility and capacity for hard coral assemblages to reorganize and maintain competitive dominance at an intra-atoll scale in response to gradients in physical drivers. Our finding that benthic regimes can switch dramatically at clearly identifiable physical thresholds adds to the growing body of evidence that coral reef communities respond in a non-linear fashion to an array of human and natural drivers. The challenge is to identify manageable drivers that compromise key ecosystem services on coral reefs in the context of unmanageable, natural physical regimes.

Acknowledgements. This work was part of an interdisciplinary effort by the NOAA Pacific Islands Fisheries Science Center's Coral Reef Ecosystem Division (CRED) to assess, understand, and monitor coral reef ecosystems of the US Pacific. The authors thank Rusty Brainard, Principal Investigator of CRED, for his support of this research. We also thank Oliver Vetter, Chip Young, Noah Pomeroy, Ronald Hoeke, and Daniel Merritt for their invaluable assistance in mooring deployments and data gathering, the CRED tow-board team, and the officers and crew of the NOAA ship *Hi'ialakai* for logistic support and field assistance. Jeff Sevadjian, Timothy Jones, Casey Wilkinson and Jessica Blakely provided important input related to data analysis, and Alan Friedlander, Jeff Drazen, Craig Smith, and Mark Merrifield provided helpful comments and guidance on this work. Funding for surveys (as part of the Pacific Reef Assessment and Monitoring Program, RAMP) was provided by NOAA's Coral Reef Conservation Program. Scripps Institution of Oceanography is a member of the Palmyra Atoll Research Consortium (PARC). This is PARC publication number PARC-0114

LITERATURE CITED

Andrews JC, Gentien P (1982) Upwelling as a source of nutrients for the Great Barrier Reef ecosystems: A solution to Darwin's question? Mar Ecol Prog Ser 8:257–269

Atkinson M, Bilger R (1992) Effects of water velocity on phosphate uptake in coral reef-flat communities. Limnol Oceanogr 37:273–279

Booij N, Ris RC, Holthuijsen LH (1999) A third-generation wave model for coastal regions: 1. Model description and validation. J Geophys Res Oceans 104:7649–7666

Bradbury RH, Young PC (1981) The effects of a major forcing function, wave energy, on a coral reef ecosystem. Mar Ecol Prog Ser 5:229–241

Brown BE (1997) Adaptations of reef corals to physical environmental stress. In: Blaxter JHS, Southward AJ (eds) Advances in marine biology, Vol 31. Academic Press, Waltham, MA, p 221–299

Chang CP, Liu CH, Kuo HC (2003) Typhoon Vamei: an equatorial tropical cyclone formation. Geophys Res Lett 30:1150–1154, doi:10.1029/2002GL016365

D'agata S, Mouillot D, Kulbicki M, Andréfouët S and others (2014) Human-mediated loss of phylogenetic and functional diversity in coral reef fishes. Curr Biol 24:555–560

DeMartini EE, Friedlander AM, Sandin SA, Sala E (2008) Differences in fish-assemblage structure between fished and unfished atolls in the northern Line Islands, central Pacific. Mar Ecol Prog Ser 365:199–215

Dollar SJ (1982) Wave stress and coral community structure in Hawaii. Coral Reefs 1:71–81

Done TJ (1999) Coral community adaptability to environmental change at the scales of regions, reefs and reef zones. Am Zool 39:66–79

Elith J, Leathwick JR, Hastie T (2008) A working guide to boosted regression trees. J Anim Ecol 77:802–813

Engelen AH, Åberg P, Olsen JL, Stam WT, Breeman AM (2005) Effects of wave exposure and depth on biomass, density and fertility of the fucoid seaweed *Sargassum polyceratium* (Phaeophyta, Sargassaceae). Eur J Phycol 40:149–158

Fabricius KE (2005) Effects of terrestrial runoff on the ecology of corals and coral reefs: review and synthesis. Mar Pollut Bull 50:125–146

Fabricius K, De'ath G, McCook L, Turak E, Williams DM (2005) Changes in algal, coral and fish assemblages along water quality gradients on the inshore Great Barrier Reef. Mar Pollut Bull 51:384–398

Franklin EC, Jokiel PL, Donahue MJ (2013) Predictive modeling of coral distribution and abundance in the Hawaiian Islands. Mar Ecol Prog Ser 481:121–132

Friedman JH, Meulman JJ (2003) Multiple additive regression trees with application in epidemiology. Stat Med 22: 1365–1381

Gove JM, Williams GJ, McManus MA, Heron SF, Sandin SA, Vetter OJ, Foley DG (2013) Quantifying Climatological Ranges and Anomalies for Pacific Coral Reef Ecosystems. PLoS ONE 8:e61974

Grigg RW (1983) Community structure, succession and development of coral reefs in Hawaii. Mar Ecol Prog Ser 11:1–14

Hamann IM, Boehlert GW, Wilson CD (2004) Effects of steep topography on the flow and stratification near Palmyra Atoll. Ocean Dyn 54:460–473

Hendry R, Wunsch C (1973) High Reynolds number flow past an equatorial island. J Fluid Mech 58:97–114

Hughes TP (1994) Catastrophes, phase-shifts, and large-scale degredation of a Caribbean coral reef. Science 265: 1547–1551

Hughes TP, Connell JH (1999) Multiple stressors on coral reefs: a long-term perspective. Limnol Oceanogr 44: 932–940

Hughes TP, Baird AH, Dinsdale EA, Moltschaniwskyj NA, Pratchett MS, Tanner JE, Willis BL (2012) Assembly rules of reef corals are flexible along a steep climatic gradient. Curr Biol 22:736–741

Jouffray JB, Nyström M, Norström AV, Williams ID, Wedding LM, Kittinger JN, Williams GJ (2015) Identifying multiple coral reef regimes and their drivers across the Hawaiian archipelago. Philos Trans R Soc B Biol Sci 370: (in press) doi:10.1098/rstb.2013.0268

Kenyon JC, Brainard RE, Hoeke RK, Parrish FA, Wilkinson CB (2006) Towed-diver surveys, a method for mesoscale spatial assessment of benthic reef habitat: a case study at Midway Atoll in the Hawaiian Archipelago. Coast Manag 34:339–349

Kilar JA, McLachlan J (1989) Effects of wave exposure on the community structure of a plant-dominated, fringing-reef platform: intermediate disturbance and disturbance-mediated competition. Mar Ecol Prog Ser 54:265–276

Kleypas JA, McManus JW, Menez LAB (1999) Environmental limits to coral reef development: Where do we draw the line? Am Zool 39:146–159

Kohler KE, Gill SM (2006) Coral Point Count with Excel extensions (CPCe): A Visual Basic program for the determination of coral and substrate coverage using random point count methodology. Comput Geosci 32:1259–1269

Leichter JJ, Miller SL (1999) Predicting high-frequency upwelling: spatial and temporal patterns of temperature anomalies on a Florida coral reef. Cont Shelf Res 19: 911–928

Leichter JJ, Shellenbarger G, Genovese SJ, Wing SR (1998) Breaking internal waves on a Florida (USA) coral reef: a plankton pump at work? Mar Ecol Prog Ser 166:83–97

Leichter JJ, Stewart HL, Miller SL (2003) Episodic nutrient transport to Florida coral reefs. Limnol Oceanogr 48: 1394–1407

Lesser GR, Roelvink JA, van Kester JATM, Stelling GS (2004) Development and validation of a three-dimensional morphological model. Coast Eng 51:883–915

Littler MM, Littler DS (1985) Factors controlling relative dominance of primary producers on biotic reefs. Proc 5th Int Coral Reef Congr, Tahiti 4:35–40

Lundblad ER, Wright DJ, Miller J, Larkin EM and others (2006) A benthic terrain classification scheme for American Samoa. Mar Geod 29:89–111

Lyzenga DR (1985) Shallow-water bathymetry using combined lidar and passive multispectral scanner data. Int J Remote Sens 6:115–125

Madin JS (2005) Mechanical limitations of reef corals during hydrodynamic disturbances. Coral Reefs 24:630–635

Madin JS, Connolly SR (2006) Ecological consequences of major hydrodynamic disturbances on coral reefs. Nature 444:477–480

Madin J, Black K, Connolly S (2006) Scaling water motion on coral reefs: from regional to organismal scales. Coral Reefs 25:635–644

Mandelbrot BB (1983) The fractal geometry of nature. WH Freeman, New York, NY

Maragos JE, Williams GJ (2011) Pacific coral reefs: an introduction. In: Hopley D (ed) Encyclopedia of modern coral reefs. Springer-Verlag, Dordrecht, p 753–776

McClanahan T, Karnauskas M (2011) Relationships between benthic cover, current strength, herbivory, and a fisheries closure in Glovers Reef Atoll, Belize. Coral Reefs 30:9–19

McClanahan TR, Graham NAJ, MacNeil MA, Muthiga NA, Cinner JE, Bruggemann JH, Wilson SK (2011) Critical thresholds and tangible targets for ecosystem-based management of coral reef fisheries. Proc Natl Acad Sci USA 108:17230–17233

McCook LJ (1999) Macroalgae, nutrients and phase shifts on coral reefs: scientific issues and management consequences for the Great Barrier Reef. Coral Reefs 18: 357–367

Meisel JE, Turner MG (1998) Scale detection in real and artificial landscapes using semivariance analysis. Landscape Ecol 13:347–362

Page-Albins KN, Vroom PS, Hoeke R, Albins MA, Smith CM

(2012) Patterns in benthic coral reef communities at Pearl and Hermes Atoll along a wave-exposure gradient. Pac Sci 66:481–496

Pebesma EJ (2004) Multivariable geostatistics in S: the gstat package. Comput Geosci 30:683–691

Plotnick RE, Gardner RH, O'Neil RV (1993) Lacunarity indices as measures of landscape texture. Landscape Ecol 8:201–211

Raubenheimer B, Guza RT (1996) Observations and predictions of run-up. J Geophys Res Oceans 101:25575–25587

Richards BL, Williams ID, Vetter OJ, Williams GJ (2012) Environmental factors affecting large-bodied coral reef fish assemblages in the Mariana Archipelago. PLoS ONE 7:e31374

Ridgeway G (2012) Generalized boosted regression models. Documentation on the R package 'gbm', version 1.6–32, www.r-project.org/

Roder C, Fillinger L, Jantzen C, Schmidt GM, Khokiattiwong S, Richter C (2010) Trophic response of corals to large amplitude internal waves. Mar Ecol Prog Ser 412: 113–128

Roder C, Jantzen C, Schmidt GM, Kattner G, Phongsuwan N, Richter C (2011) Metabolic plasticity of the corals *Porites lutea* and *Diploastrea heliopora* exposed to large amplitude internal waves. Coral Reefs 30:57–69

Sandin SA, Smith JE, DeMartini EE, Dinsdale EA and others (2008) Baselines and degradation of coral reefs in the Northern Line Islands. PLoS ONE 3:e1548

Sevadjian JC, McManus MA, Benoit-Bird KJ, Selph KE (2012) Shoreward advection of phytoplankton and vertical re-distribution of zooplankton by episodic near-bottom water pulses on an insular shelf: Oahu, Hawaii. Cont Shelf Res 50–51:1–15

Smith JE, Smith CM, Vroom PS, Beach KL, Miller S (2004) Nutrient and growth dynamics of Halimeda tuna on Conch Reef, Florida Keys: possible influence of internal tides on nutrient status and physiology. Limnol Oceanogr 49:1923–1936

Sousa WP (1984) The role of disturbance in natural communities. Annu Rev Ecol Syst 15:353–391

Storlazzi CD, Brown EK, Field ME, Rodgers K, Jokiel PL (2005) A model for wave control on coral breakage and species distribution in the Hawaiian Islands. Coral Reefs 24:43–55

Thomas FIM, Atkinson MJ (1997) Ammonium uptake by coral reefs: effects of water velocity and surface roughness on mass transfer. Limnol Oceanogr 42:81–88

Tomczak M, Godfrey JS (1994) Regional oceanography: an introduction. Pergamon, New York, NY

Vroom P, Musburger C, Cooper S, Maragos J, Page-Albins K, Timmers MV (2010) Marine biological community baselines in unimpacted tropical ecosystems: spatial and temporal analysis of reefs at Howland and Baker Islands. Biodivers Conserv 19:797–812

Williams GJ, Maragos JE, Davy SK (2008) Characterization of the coral communities at Palmyra Atoll in the remote Central Pacific. Atoll Res Bull 557:1–30

Williams GJ, Knapp IS, Maragos JE, Davy SK (2010) Modeling patterns of coral bleaching at a remote Central Pacific atoll. Mar Pollut Bull 60:1467–1476

Williams GJ, Knapp IS, Aeby GS, Davy SK (2011a) Spatial and temporal patterns of scleractinian coral, soft coral, and zoanthid disease on a remote, near-pristine coral reef (Palmyra Atoll, central Pacific). Dis Aquat Org 94: 89–100

Williams GJ, Knapp IS, Maragos JE, Davy SK (2011b) Proximate environmental drivers of coral communities at Palmyra Atoll: establishing baselines prior to removing a WWII military causeway. Mar Pollut Bull 62:1842–1851

Williams GJ, Smith JE, Conklin EJ, Gove JM, Sala E, Sandin SA (2013) Benthic communities at two remote Pacific coral reefs: effects of reef habitat, depth, and wave energy gradients on spatial patterns. PeerJ 1:e81

Williams GJ, Gove JM, Eynaud Y, Zgliczynski B, Sandin SA (in press) Local human impacts decouple natural biophysical relationships on Pacific coral reefs. Ecography doi:10.1111/ecog.01353

Wolanski E, Delesalle B (1995) Upwelling by internal waves, Tahiti, French Polynesia. Cont Shelf Res 15:357–368

Wooldridge SA (2009) Water quality and coral bleaching thresholds: formalising the linkage for the inshore reefs of the Great Barrier Reef, Australia. Mar Pollut Bull 58: 745–751

Wright DJ, Pendleton M, Boulware J, Walbridge S and others (2012) Benthic Terrain Modeler. Book v. 3.0. Environmental Systems Research Institute, NOAA Coastal Services Center, Massachusetts Office of Coastal Zone Management, Boston, MA

Editorial responsibility: Tim McClanahan, Mombasa, Kenya

Submitted: April 14, 2014; Accepted: November 12, 2014
Proofs received from author(s): February 6, 2015